FIELD-EFFECT TRANSISTOR BASED ON GRAPHENE — POROUS SILICON HYBRID STRUCTURE

I. B. Olenych, Ya. V. Boyko
Ivan Franko National University of Lviv,
50, Drahomanov St., Lviv, 79005, Ukraine,
e-mail: igor.olenych@lnu.edu.ua

(Received 28 October 2022; in final form 23 January 2023; accepted 24 January 2023; published online 04 March 2023)

In this study, reduced graphene oxide (rGO) — porous silicon (PS) hybrid structures are suggested to create a field-effect transistor (FET). The electrical properties and switching characteristics of the obtained rGO–PS-based FET were studied in both DC and AC modes. A significant influence of the supporting PS layer on the transport of charge carriers in the graphene film was established. A decrease in resistance and an increase in the capacity of the graphene FET channel due to photogenerated charge carriers in the porous layer were found. Based on the impedance spectra, the parameters of the equivalent circuit model of the rGO–PS-based FET for different gate voltages are determined.

Key words: field-effect transistor, graphene, porous silicon, hybrid structure, current-voltage characteristics, impedance.

DOI: https://doi.org/10.30970/jps.27.1701

I. INTRODUCTION

Since the discovery of the influence of an electric field on the conductivity of graphene [1], a large number of field-effect transistors (FETs) using graphene as a channel material have been researched. Graphene FETs are recognized as a potential alternative to metal-oxide-semiconductor transistors and can be building blocks for next-generation electronic devices in the post-silicon epoch. Intensive research and development of graphene-based electronics is due to the unique properties of the carbon 2D material. The extremely high mobility of charge carriers and high electrical conductivity of graphene due to the gapless cone-shaped energy structure is a significant advantage of the material for creating high-speed devices [2–4]. Another potential advantage of graphene is the ability to withstand significant current density, which, together with high thermal conductivity and an Ohmic contact with metals, makes graphene FETs promising for use in high-power circuits [5–7]. The outstanding mechanical properties of graphene have the potential for application in nanoelectromechanical systems [8, 9]. The 98% transparency of graphene is ideal for creating optically transparent electrodes for photodetectors, solar cells, flexible displays, and other optoelectronic devices [10–12].

Various sensor devices for physical, chemical, and biological applications have been developed on the basis of graphene FETs [13, 14]. Recently considerable attention has been focused on the use of graphene FETs in radio-frequency electronics [15]. However, most of the potential applications of graphene are still in the development, verification and industrial scale-up stages. In addition, the potential for practical use of the unique properties of graphene is far from fully revealed. A number of obstacles have to be overcome before the mass production of graphene-based devices becomes a reality. In particular, a weak point of graphene FETs is the switching characteristic, namely the ratio of the current in the on-state to the current in the off-state (I_{on}/I_{off}). This imperfection caused by the zero band gap of graphene can be eliminated if a graphene nanoribbon is used as the FET channel [16, 17]. Due to the lateral quantum confinement, the band gap opens in the electronic structure of the graphene nanoribbon as a quasi-1D system. In addition, a small band gap was discovered in bilayer graphene [18, 19], which enhances the prospect of developing graphene-based FETs. On the other hand, localized states in the supporting dielectric and at the graphene/dielectric interface have an important influence on carrier mobility in the graphene channel. In particular, electrically active defects in the surface layer of silicon oxide can be charged and discharged through the graphene channel and can be centers of carrier scattering. Optimizing the interface between graphene nanosheets and the supporting dielectric can increase the efficiency of electronic devices [20, 21]. From this point of view, studies of various types of supporting layers of graphene FETs can be promising.

Due to the sponge-like structure, porous silicon (PS) is recognized as an attractive substrate material for the deposition of graphene nanosheets [22]. It is simple to control the morphology and state of the surface of the porous layer [23] and thereby influence the electronic processes in the graphene film. In addition, using photoluminescence attenuation of the PS nanostructures, the number of graphene layers in the film can be estimated in situ. The PS–graphene sandwich-like structures have a high potential for use in photodetectors, gas sensors, and energy conversion devices [22, 24–26]. In this work, we used hybrid structures in order to create the graphene-based FET and investigate the features of charge transfer processes in alternating and direct current modes.

II. EXPERIMENT

Graphene-based FETs were created by depositing reduced graphene oxide (rGO) nanosheets on the PS surface. Layers of the nanostructured PS on silicon wafers were formed using the electrochemical etching technology. Silicon wafers of electronic conductivity type with a thickness of 400 µm and crystallographic orientation [100] were used. The PS layer homogeneity was achieved by thermal deposition of Au film about 0.5 µm thick on the back surface of the silicon wafer. After annealing at 450°C for 20 min, the Au film also served as a gate contact for further measurements. An ethanol solution of hydrofluoric acid with $C_2H_5OH : HF = 1 : 1$ volume ratio was used as an electrolyte. The anodic current density was about 30 mA/cm^2 during the 5 min etching process. Besides, the working surface of the silicon wafer was irradiated by the 500 W filament lamp to generate holes in the n-Si near-surface layer the necessary for etching. The PS samples obtained as a result of etching were washed with distilled water and dried at room temperature.

The 2 mg/ml aqueous suspension of graphene oxide (GO) produced by Biotool (Germany) was used to obtain graphene nanosheets. The GO suspension was dispersed by ultrasonic treatment for 10–20 min and reduced with hydrazine monohydrate. The 0.2 M aqueous solution of sodium dodecylbenzene sulfonate was used to prevent the aggregation of the obtained rGO nanoparticles. The rGO dispersion was deposited on the PS surface. After drying at room temperature, the rGO nanosheets formed a film for the channel FET. As a result, the rGO–PS hybrid structures were obtained. The source and drain of the FET were formed by thermal deposition on the rGO film of Ag contacts. The distance between these contacts was 1 mm. Metallic films provide reliable contact with the PS and rGO nanostructures [24, 27]. A schematic representation of the obtained FET based on the rGO–PS hybrid structure is shown in Figure 1. The linear dimensions of the experimental samples were 3×3 mm.

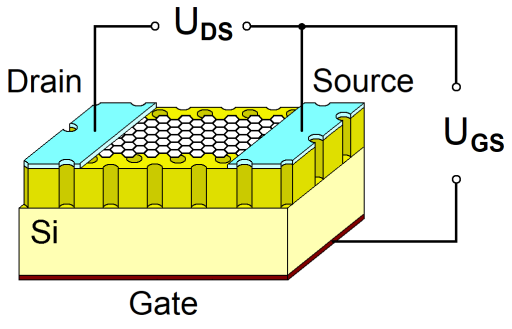

Fig. 1. Schematic representation of the FET based on the rGO–PS hybrid structure

The electrical characteristics of the obtained structures were studied in both DC and AC modes. The current-voltage characteristics (CVCs) were measured when the current passed between the source and drain contacts. The gate voltage of different magnitudes and signs was applied additionally as shown in Fig. 1. Impedance spectroscopy of the experimental structures was performed using the source and drain contacts by RLC measuring device in the 25 Hz–1 MHz frequency range. Photoelectric phenomena were studied by irradiating the rGO–PS hybrid structures from the side of the graphene layer with the 1 W white LED (FYLP–1W–UWB–A) that provided a light flux of 76 lumens. All measurements were carried out at room temperature.

III. RESULTS AND DISCUSSION

The CVCs of the rGO film deposited on the PS surface are shown in Fig. 2. The measured dependencies of drain current I_{DS} on drain-source voltage U_{DS} are nonlinear, which indicates complex charge transfer processes in hybrid structures. Considering that graphene is characterized by the Ohmic contact resistance with metals [5], it can be assumed that the nonlinear CVCs of the FETs based on the rGO–PS structures are caused by the influence of the supporting PS layer. In particular, the electrical conductivity of the rGO film can be caused by charge carriers injected not only from contacts but also from the PS nanostructures. Despite the high resistance of the porous layer compared to the bulk material, the PS cannot be considered an ideal dielectric. Therefore, the gate voltage application does not only change the Fermi level position in the conical electronic structure of graphene and, as a result, the conductivity of the rGO film, but also causes the transfer of free charge carriers through the porous layer and the silicon substrate. Taking into account the electronic conductivity of the supporting PS layer, the resulting transfer characteristic of the FET also depends on the gate voltage sign, which determines the n- or p-type of the rGO film conductivity. The above processes cause the moving of the CVCs along the U_{DS} axis and different values of the forward and reverse currents under the influence of the gate-source voltage U_{GS} of both negative and positive signs (see Fig. 2).

An important characteristic of graphene FETs is the drain current I_{DS} dependence on the gate voltage U_{GS}. As can be seen in Fig. 3, the measured I_{DS}–U_{GS} dependencies have linear sections, whose position depends on the sign and magnitude of the U_{DS}. It is possible to change the channel conductivity of the graphene FET based on the rGO–PS hybrid structures by more than two orders of magnitude by changing the gate voltage. The obtained I_{DS}–U_{GS} dependencies did not reveal a pronounced Dirac point, i. e., the minimum in the graphene film conductivity in the case when the Fermi level passes through the point of contact of the cone-shaped conduction and valence bands. This feature of PS-supporting devices can be due to the charge transfer through the porous layer and the formation of electrical barriers at the PS/rGO film interface, which prevent the injection of free charge carriers of the sign corresponding to the gate voltage into the graphene.

In addition, the performance of graphene FETs si-

gnificantly depends on trapped charge effects in the supporting layer [21]. It should be noted that the PS nanostructures have trapping levels of various natures with quasi-continuous energy distribution [28]. Therefore, the local electric field of trapped charges in the porous layer significantly affects the drain current. An additional confirmation of this hypothesis is an increase in the conductivity of the channel of the FETs based on the rGO–PS structures under the influence of white light irradiation (see Fig. 4). Photogenerated in the PS layer electron-hole pairs can probably change the concentration of charge carriers in the rGO film not only due to injection but also due to their local field. As a result, the rGO–PS-based FETs show a decrease in the resistance and an increase in the electric capacity of the channel under the influence of light in the AC mode.

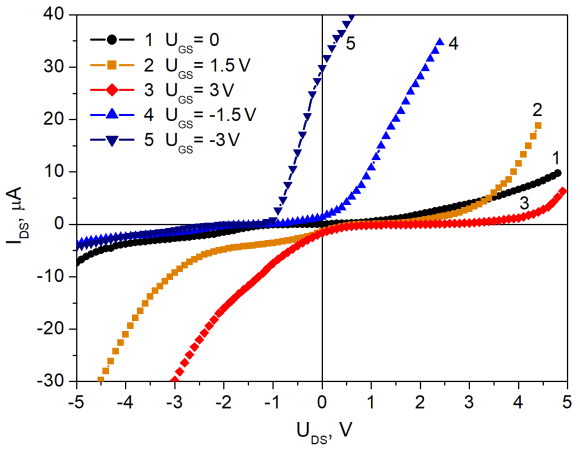

Fig. 2. The CVCs of the FET based on the rGO–PS structure for different gate-source voltage U_{GS}

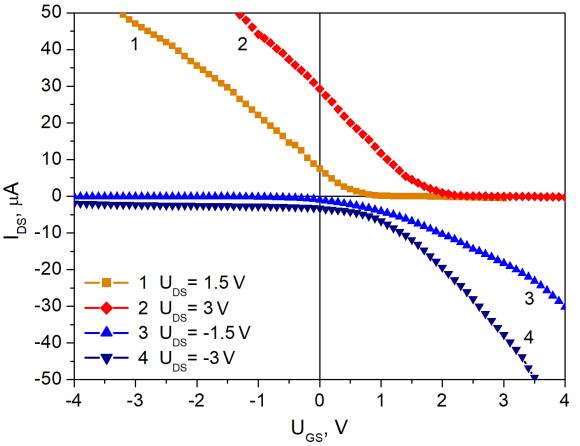

Fig. 3. The dependencies of drain current I_{DS} on gate-source voltage U_{GS} of the FET based on the rGO–PS structure for different drain-source voltage U_{DS}

Besides, the frequency dependencies of the impedance were measured to study the features of the charge transport processes in the FETs based on the rGO–PS structures. As can be seen in Fig. 4, the hybrid structures show a decrease in internal resistance and electrical capacitance with increasing frequency. Figure 5 presents Nyquist plots of the rGO–PS-based field-effect devices in the complex plane $Z_{\mathrm{Re}} - Z_{\mathrm{Im}}$.

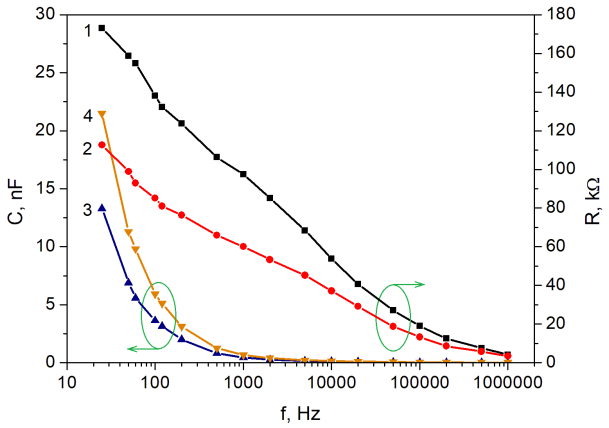

Fig. 4. Frequency dependence of the electrical resistance (curves 1,2) and the capacitance (curves 3,4) of the rGO–PS-based FET obtained in the dark (curves 1, 3) and under irradiation by the 1 W white LED (curves 2, 4)

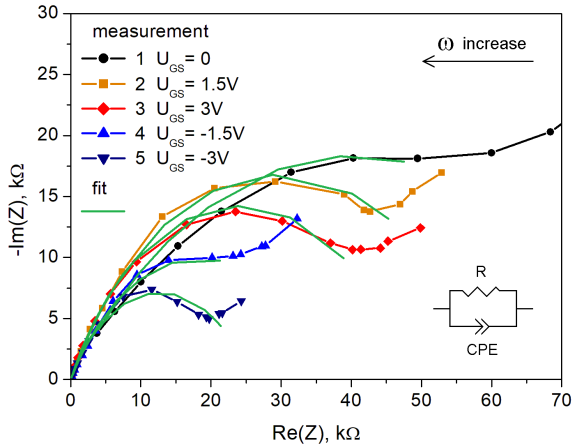

Fig. 5. Nyquist plots and equivalent circuit diagram of the rGO–PS-based FET channel for different gate-source voltage U_{GS}

An equivalent circuit model was constructed to interpret the impedance. It is advisable to use an approach that has proven itself well in the case of fractal and composite materials for constructing an impedance model hybrid structure [24, 29, 30]. Within our model, the resistive-capacitive properties of the FET channel in the frequency range of 200 Hz–1 MHz are best described using the composition of a parallel-connected constant phase element (CPE) and a resistor with the resistance R. The expression for the impedance of the R–CPE model will be as follows:

$$Z(\omega) = \frac{R}{1 + (j\omega)^n RQ},$$

where Q is the CPE and n characterizes the heterogeneity of the electrical properties of the hybrid structure. In the case $n = 1$, CPE is associated with an ideal

capacitor and when $n = 0$, CPE transforms into a pure resistor. A reliable interpretation of the low-frequency range of impedance, which usually corresponds to the process of charge carrier transfer through the boundary of nanoparticles, needs more experimental data and additional research at even lower frequencies. The values of resistance and CPE parameters obtained as a result of the impedance spectra approximation in the 200 Hz–1 MHz frequency range are shown in Table 1.

Gate voltage U_{GS}, V	Parameters of approximation		
	R, kΩ	$Q\times10^{-8}$	n
0	80.689	3.34	0.543
1.5	59.525	9.09	0.654
3	48.228	5.57	0.679
−1.5	36.700	23.64	0.631
−3	25.446	16.47	0.649

Table 1. The approximation parameters of the impedance spectra of the FET based on the rGO–PS structure

The effect of the gate voltage caused the drop in the internal resistance and improved capacitive properties of the channel of the FET based on the rGO–PS structure due to a change in the concentration of free charge carriers in the rGO film. Moreover, larger changes in electrical characteristics of the FET are observed for negative gate voltage, which may be related to the influence of the supporting PS layer.

IV. CONCLUSIONS

In this study, we focused on novel technical solutions relevant to the design of graphene FETs. The rGO–PS hybrid structures for FETs were created by electrochemical etching of silicon wafers and deposition on the porous layer of graphene nanosheets from water dispersion. Based on the analysis of CVCs of the obtained structures, a significant influence of the supporting PS layer on the conductivity of the graphene FET channel was established. Linear sections with the I_{on}/I_{off} ratio exceeding 100 were detected on the dependencies of the drain current on the gate voltage.

We have found a decrease in electrical capacitance and internal resistance of the rGO–PS structures with an increase in the frequency from 25 Hz to 1 MHz. In addition, the research structures demonstrate an increase in conductivity and capacity under the action of white light irradiation. The internal resistance and CPE parameters of hybrid structures were determined using the approximation of the impedance spectra. It was shown that the impact of gate voltage on the electrical characteristics of the rGO–PS structures manifests a decrease in the internal resistance of the graphene FET channel. The obtained results can be used to design field-effect devices based on graphene.

[1] K. S. Novoselov *et al.*, Science **306**, 666 (2004); https://doi.org/10.1126/science.1102896.

[2] S. Fratini, F. Guinea, Phys. Rev. B **77**, 195415 (2008); https://doi.org/10.1103/PhysRevB.77.195415.

[3] K. Erickson *et al.*, Adv. Mater. **22**, 4467 (2010); https://doi.org/10.1002/adma.201000732.

[4] K. I. Bolotin *et al.*, Solid State Commun. **146**, 351 (2008); https://doi.org/10.1016/j.ssc.2008.02.024.

[5] F. Xia, V. Perebeinos, Y.-M. Lin, Y. Wu, P. Avouris, Nature Nanotech. **6**, 179 (2011); https://doi.org/10.1038/nnano.2011.6.

[6] A. K. Geim, Science **324**, 1530 (2009); https://doi.org/10.1126/science.1158877.

[7] K. M. F. Shahil, A. A. Balandin, Solid State Commun. **152**, 1331 (2012); https://doi.org/10.1016/j.ssc.2012.04.034.

[8] C. Lee, X. Wei, J. W. Kysar, J. Hone, Science **321**, 385 (2008); https://doi.org/10.1126/science.1157996.

[9] J. S. Bunch *et al.*, Science **315**, 490 (2007); https://doi.org/10.1126/science.1136836.

[10] K. S. Kim *et al.*, Nature **457**, 706 (2009); https://doi.org/10.1038/nature07719.

[11] F. Xia, T. Mueller, Y.-M. Lin, A. Valdes-Garcia, P. Avouris, Nature Nanotech. **4**, 839 (2009); https://doi.org/10.1038/nnano.2009.292.

[12] P. Avouris, Nano Lett. **10**, 4285 (2010); https://doi.org/10.1021/nl102824h.

[13] B. Zhan *et al.*, Small **10**, 4042 (2014); https://doi.org/10.1002/smll.201400463.

[14] S. Wu, Q. He, C. Tan, Y. Wang, H. Zhang, Small **9**, 1160 (2013); https://doi.org/10.1002/smll.201202896.

[15] J.-S. Moon, Carbon Lett. **13**, 17 (2012); https://doi.org/10.5714/CL.2012.13.1.017.

[16] S. Lone, A. Bhardwaj, A. K. Pandit, S. Gupta, S. Mahajan, J. Electron. Mater. **50**, 3169 (2021); https://doi.org/10.1007/s11664-021-08859-y.

[17] M. Y. Han, B. Ozyilmaz, Y. Zhang, P. Kim, Phys. Rev. Lett. **98**, 206805. (2007); https://doi.org/10.1103/PhysRevLett.98.206805.

[18] T. Ohta, A. Bostwick, T. Seyller, K. Horn, E. Rotenberg, Science **313**, 951 (2006); https://doi.org/10.1126/science.1130681.

[19] E. McCann, D. S. L. Abergel, V. I. Fal'ko, Eur. Phys. J. Spec. Top. **148**, 91 (2007); https://doi.org/10.1140/epjst/e2007-00229-1.

[20] K. Nagashio, T. Yamashita, T. Nishimura, K. Kita, A. Toriumi, J. Appl. Phys. **110**, 024513 (2011); https://doi.org/10.1063/1.3611394.

[21] G. Imamura, K. Saiki, ACS Appl. Mater. Interfaces **7**, 2439 (2015); https://doi.org/10.1021/am5071464.

[22] J. Kim *et al.*, ACS Appl. Mater. Interfaces **6**, 20880 (2014); https://doi.org/10.1021/am5053812.

[23] H. Föll, M. Christophersen, J. Carstensen, G. Hasse,

Mater. Sci. Eng. R Rep. **39**, 93 (2002); https://doi.org/10.1016/S0927-796X(02)00090-6.

[24] I. B. Olenych, O. I. Aksimentyeva, L. S. Monastyrskii, Yu. Yu. Horbenko, M. V. Partyka, Nanoscale Res. Lett. **12**, 272 (2017); https://doi.org/10.1186/s11671-017-2043-7.

[25] I. B. Olenych, L. S. Monastyrskii, O. I. Aksimentyeva, L. Orovcík, M. Y. Salamakha, Mol. Cryst. Liq. Cryst. **673**, 32 (2018); https://doi.org/10.1080/15421406.2019.1578491.

[26] L. Oakes *et al.*, Sci. Rep. **3**, 3020 (2013); https://doi.org/10.1038/srep03020.

[27] I. B. Olenych, O. I. Aksimentyeva, Yu. Yu. Horbenko, B. R. Tsizh, Appl. Nanosci. **12**, 579 (2022); https://doi.org/10.1007/s13204-021-01698-7.

[28] I. Olenych, B. Tsizh, L. Monastyrskii, O. Aksimentyeva, B. Sokolovskii, Solid State Phenom. **230**, 127 (2015); https://doi.org/10.4028/www.scientific.net/SSP.230.127.

[29] I. Karbovnyk *et al.*, Ceram. Int. **42**, 8501 (2016); https://doi.org/10.1016/j.ceramint.2016.02.075.

[30] I. Karbovnyk, H. Klym, D. Chalyy, I. Zhydenko, D. Lukashevych, Appl. Nanosci. **12**, 1263 (2022); https://doi.org/10.1007/s13204-021-01810-x.

ПОЛЬОВИЙ ТРАНЗИСТОР НА ОСНОВІ ГІБРИДНОЇ СТРУКТУРИ ҐРАФЕН–ПОРУВАТИЙ КРЕМНІЙ

І. Б. Оленич, Я. В. Бойко
Львівський національний університет імені Івана Франка,
вул. Драгоманова, 50, Львів, 79005, Україна

У роботі запропоновано сандвіч-структури на основі відновленого оксиду ґрафену (rGO) та поруватого кремнію (PS) для створення ґрафенового польового транзистора. Гібридні структури rGO–PS виготовлені методом фотоелектрохімічного травлення кремнієвих пластин та осадженням на поверхню PS нанолистів ґрафену, одержаних відновленням водної суспензії оксиду ґрафену моногідратом гідразину. Електричні властивості та характеристики перемикання польового транзистора на основі структури rGO–PS досліджено в режимах сталого та змінного струму. Аналіз ВАХ одержаних структур засвідчує значний вплив шару PS, який розділяє плівку rGO з електродом затвора, на перенесення носіїв заряду в ґрафенових наночастинках. На залежностях струму стоку від напруги на затворі виявлено лінійні ділянки, розташування яких залежить від різниці потенціалів між витоком і стоком досліджуваного транзистора. Комутаційні властивості польового транзистора на основі структури rGO–PS характеризуються зміною провідності ґрафенової плівки більш ніж на два порядки внаслідок зміни напруги на затворі.

За допомогою імпедансної спектроскопії зареєстровано зменшення електричної ємності та внутрішнього опору структур rGO–PS зі збільшенням частоти від 25 Гц до 1 МГц і збільшення провідності та ємності під впливом опромінення білим світлом, яке зумовлене фотоґенерованими носіями заряду в порувату шарі. На основі спектрів імпедансу визначено параметри моделі еквівалентної схеми польового транзистора на основі структури rGO–PS для різних напруг на затворі. Продемонстровано, що збільшення різниці потенціалів між витоком і затвором зменшує внутрішній опір плівки rGO. Отримані результати можуть бути використані для розробки пристроїв на основі гібридних структур rGO–PS, робота яких ґрунтується на ефекті поля.

Ключові слова: польовий транзистор, ґрафен, поруватий кремній, гібридна структура, вольтамперна характеристика, імпеданс.